Integrating kinetic models, gene circuits, and biofilm dynamics for enhanced exopolysaccharide production in nitrifying bacterial consortia

Indhuja Sakthivel, Boobal Rangaswamy, Bharathkumar Rajagopal, Lathika Shanmugam

PII: S0167-7012(25)00153-8

DOI: https://doi.org/10.1016/j.mimet.2025.107237

Reference: MIMET 107237

To appear in: *Journal of Microbiological Methods*

Received date: 22 April 2025

Revised date: 18 August 2025

Accepted date: 21 August 2025

Please cite this article as: I. Sakthivel, B. Rangaswamy, B. Rajagopal, et al., Integrating kinetic models, gene circuits, and biofilm dynamics for enhanced exopolysaccharide production in nitrifying bacterial consortia, *Journal of Microbiological Methods* (2024), https://doi.org/10.1016/j.mimet.2025.107237

Integrating Kinetic Models, Gene Circuits, and Biofilm Dynamics for Enhanced Exopolysaccharide Production in Nitrifying Bacterial Consortia

Indhuja Sakthivel[1], Boobal Rangaswamy[1]*, Bharathkumar Rajagopal[2], Lathika Shanmugam[1]

[1]*Department of Biotechnology, PSG College of Arts & Science, Coimbatore, Tamil Nadu 641014, India*

[2]*Amity Institute of Biotechnology, Amity University Uttar Pradesh, Noida 201313, India*

*Corresponding author. E-mail address: boobal@psgcas.ac.in (Boobal Rangaswamy)

ORCID: 0000-0002-8270-9755 (Boobal Rangaswamy); 0009-0006-1322-4515 (Lathika Shanmugam); ORCID: 0000-0002-7922-8467 (Bharathkumar Rajagopal)

Abstract

Bacterial consortia enriched from domestic wastewater were studied through kinetic and genetic circuit modeling to optimize extracellular polysaccharide (EPS) production and nitrogen removal. This study integrates kinetic modelling and synthetic biology to optimize consortia performance. Growth kinetics were simulated using extended Monod and Verhulst models, under controlled nitrogen flux (10 ppm NH_4Cl), yielding a maximum biomass concentration (OD_{590} = 5.39) and an EPS production of 2.63 g/L by day 45. The Monod model described the specific growth rate (μ) as a function of nitrogen concentration (S_n), while the Verhulst model estimated biomass accumulation over time. Scanning electron microscopy (SEM) showed the gradual development of biofilms, starting from scattered clusters, and progressing to dense structures. Nitrogen flux analysis revealed that 80% of ammonia was oxidized by autotrophic bacteria (AOB/NOB). PCR amplification confirmed the presence of the exoY gene, which was used to build a BUFFER-gate logic gene circuit for controlling succinoglycan production. Through focused genetic and kinetic optimization, this study demonstrates effective nitrification, providing a strong framework for wastewater treatment and biofilm engineering.

Keywords: EPS, Nitrite-oxidizing bacteria, Ammonia-oxidizing bacteria, Monod model, Verhulst model, exoY

1. Introduction

Over the past few decades, environmental biologists and microbiologists have used microbial resources for wastewater treatment. Earlier studies used a single-strain microorganisms that produced notable results (Song et al., 2021). Subsequent research has suggested that mixed microbial consortia may provide a more sustainable approach to wastewater remediation (both metals and organics) than single-strain treatments. These dynamic bacterial assemblages are being used in many ways for their ability to remove pollutants, especially in biological wastewater treatment systems. By using their high biodegradation efficiency to degrade contaminants, microbial consortia provide an economical and environmentally responsible substitute for traditional wastewater treatment methods. Moreover, the consortium helps to enhance wastewater quality by decreasing the odor and color, thereby improving the performance and sustainability of treatment plants (Del Nery et al., 2016). Bacterial biofilm improves operational sustainability in large-scale wastewater treatment systems by reducing sludge formation in contrast to conventional techniques such as chemical treatments and membrane filtration (He et al., 2023). EPS is essential for biofilm activity in biological treatment systems. They affect adsorption, flocculation, settling, dewatering, and the structural integrity of microbial aggregates (Sheng et al., 2010). The extracellular matrix of bacterial biofilms mostly consists of exopolysaccharides, proteins, nucleic acids, and dead cells, playing a key role in cell-cell communication (Heilmann & Götz, 2009). Surface morphology and functionalization are also key factors in pollutant removal (Rehan et al., 2023). The development of microbial consortia is a complex process, involving multiple bacterial species that grow on surfaces and produce EPS. Chen et al. (2021) identified common biofilm-forming bacteria such as *Pseudomonas aeruginosa*, *Staphylococcus epidermidis*, *Escherichia coli*, *Klebsiella pneumoniae*, *Proteus mirabilis*, *Streptococcus viridans*, *Staphylococcus aureus*, and *Enterococcus faecalis*. Although proteins and polysaccharides are the main components of the biofilms formed by these bacteria, EPS also contains uronic acids, humic substances, lipids, and various inorganic elements (Guibaud et al., 2012; Zhao et al., 2019). These substances not only contribute to structural integrity but also help bind pollutants, which are important in designing advanced adsorbent materials (Awual et al., 2019). According to Freire-Nordi et al. (2005), EPS with uronic acids and sulphates can trap positively charged metal ions, making it useful for water purification. The composition and concentration of EPS in sludge aggregates depend on several factors, including the sludge source, type of wastewater, and operational conditions (Yuan et al., 2017). EPS has shown potential in environmental remediation by facilitating the removal of pollutants and heavy metals from contaminated areas. The consortium-associated EPS plays a significant role in cleaning up the environment (Bhattacharya et al., 2019; Hasan et al., 2021). This study supports larger environmental engineering objectives to develop sustainable systems for water purification and contaminant removal. Given its diverse functions, EPS is increasingly recognized as a key component in sustainable production systems and circular bioeconomy (Awual et al., 2019; Hasan et al., 2021).

Nitrifying bacteria, such as ammonia-oxidizing bacteria (AOB) and nitrite-oxidizing bacteria (NOB), are typically autotrophic and play a key role in nitrogen removal. Microbial consortia that include these bacteria can aid in the removal of heavy metals and nutrients (phosphate and nitrate) from the wastewater and stabilize the downstream treatment process. Similar to engineered material systems designed to both detect and remove contaminants, nitrifying bacterial consortia exhibit a dual functionality: they remove nitrogenous and metal pollutants while simultaneously detecting and responding to environmental signals through regulatory gene circuits and EPS-mediated biofilm dynamics (Awual et al., 2016); (Flemming et al., 2010). Autotrophic bacteria obtain energy by oxidizing ammonia to nitrite and then to nitrate or by using organic substances as a nitrogen source (Vajda et al., 2011; Xia et al., 2019). Nitrifying consortia also boost EPS production due to their role in microbial granulation and environmental adaptability. These factors contribute to the stability and efficiency of wastewater treatment processes, making nitrifying consortia particularly effective in EPS enhancement (Li et al., 2020; Song et al., 2020).

In bioremediation, the roles of AOB and NOB have been studied using both physiological and molecular in situ methods (Cai et al., 2018). Since several genes are involved in EPS synthesis (exo, epsE, eps9F, epsH, and epsF) contribute to the formation of the consortium structure, they are also crucial for its development (Janczarek, 2011). In a recent research, Wang et al. (2023) reported that the EPS from *Streptococcus thermophilus* has a significant application in the dairy industry and probiotics. A profound knowledge of EPS production can help to correlate the fermentation processes to improve the quality of the fermented products. Thus, the microbial EPS has broader perspectives, roles and applications in diverse bacteria. Additionally, studies confirm that nutrient sources play a major role in the production of microbial EPS. Therefore, understanding how specific genes and nutrient sources affect EPS production could improve wastewater treatment efficiency (Wang et al., 2025).

Various mathematical models have been proposed to describe changes in compound metabolism when exposed to microbial cultures from natural environments (Smith et al., 1997). Such modelling efforts are essential for optimizing performance in both biological and material-based treatment systems (Awual et al., 2020). According to Hwi Jeong and Min Lee (2013), most growth models rely on Monod kinetics and require the measurement of several parameters. The Monod model is widely used to demonstrate growth-linked substrate utilization. Additionally, Liu (2006) highlighted the Monod equation as a highly effective model for demonstrating the relationship between specific growth rate and required substrate concentration. Ruiz et al. (2013) simulated bacterial biomass growth rate using the Verhulst kinetic model. Additionally, Dmitry et al. (2015) also used the Verhulst logical equation for modelling the biomass cultivation process. This research aims to enhance the productivity of wastewater treatment plants by integrating the Monod and Verhulst models for consortium bacterial growth. The highest biomass concentration of EPS-producing species significantly increases the consortium growth which occurs at the biofilm-liquid interface (Kreft & Wimpenny, 2001). The Monod/Verhulst model has proven effective in capturing the complex non-linear dynamics of microbial

EPS production, which traditional single-factor models often fail to predict accurately (Marques et al., 2017; Plattes & Lahore, 2023). The gene circuit model, based on logic gate design principles, represents a significant advancement in synthetic biology (Lezia et al., 2022). In this framework, genetic components such as promoters, repressors, and regulatory proteins are engineered to function analogously to electronic circuits, where logic operations (e.g., AND, OR, NOT) regulate gene expression in a predictable manner. Importantly, when applied to EPS synthesis, such circuits enable the fine-tuned regulation of key biosynthetic genes, allowing for optimized flux through metabolic pathways. This integration of gene circuit engineering with microbial consortia dynamics offers a powerful strategy to enhance EPS production in nitrifying bacteria (Awual, 2016). In this study, we worked on designing a Boolean logic model to understand how to control EPS production by regulating the expression of specific genes. This allows bacteria to respond to environmental signals and improve EPS output by making better use of nitrogen sources. Overall, improving substrate flux kinetics and the construction of gene circuits can increase the efficiency of EPS production in microbial consortia. These approaches also support broader goals in developing sustainable energy and environmental technologies (Islam, Malek, et al., 2025). Hence, this study aims to construct a gene circuit based on logic gates for the EPS pathway in consortia-forming bacteria and to assess their growth kinetics, structural properties, and wastewater treatment potential.

2. Materials and methods

2.1 Sample collection and Synthetic medium preparation

The sludge sample was collected from the domestic wastewater treatment plant in Coimbatore. The sample was transferred to the lab and stored at 4°C. Modified synthetic media was prepared following 0.3g KCl, 0.5g KH_2PO_4, 2.5g NaCl, 0.02g NH_4Cl, 0.04g K_2HPO_4, 1.6g Na_2CO_3, 0.03g $CaCO_3$, 0.5g $CaCl_2$, and 5g starch (Youssef et al., 2016). The sample-inoculated culture flasks were placed in a shaker incubator at 37°C with a shaking speed of 150 rpm. Throughout the study period, the pH was maintained at an optimal value of 7.8.

The basic characterization of the wastewater physiochemical parameters was determined for the Chemical oxygen demand (COD), Biological oxygen demand (BOD), turbidity, pH, electrical conductivity, Total solids, total suspended solids (TSS) and total dissolved solids (TDS).

2.2 Consortia development

The culture was enriched with NH_4Cl of 10 ppm every two days. This addition provides the microorganisms with a nitrogen source that is expected to promote the formation of nitrogen utilizing population. The growth of the bacterial consortia was regularly measured in triplicate via optical density (OD through a UV-VIS spectrophotometer at 600 nm) and growth kinetics were systematically determined using batch culture experiments, analysed with mathematical models like Monod and Verhulst equations (Hamzah et al., 2013). To avoid spectrophotometer saturation for cultures exceeding the instrument's linear range (OD $\geq$2.2), all high-density samples were diluted before OD measurement.

The samples were diluted with sterile medium before reading and the measured OD was back-calculated for the undiluted culture. Blank corrections were performed using sterile medium. The increase in the growth ratio correlated with the increase in the biomass of the culture.

2.3 Mathematical modelling and kinetic expression of consortia growth

This study aimed to predict the consortia development by employing the mathematical model (Sadiq et al., 2018) and focused specifically on nitrogen utilization as a substrate. The Monod model expressed growth kinetics utilizing the relationship between growth and substrate concentration.

$$\mu = \mu_{max}\left[\frac{Si}{k_i+S_i}\right] \qquad (1)$$

Where the specific growth rate is represented by μ, the substrate concentration is denoted as S_i, μ_{max} stands for the maximum specific growth rate and the saturation constant is k_i. Since focused solely on a single substrate type, the specific growth rate, μ can be expressed as

$$\mu=\mu_{max}\left[\frac{S_N}{K_N+S_N}\right] \qquad (2)$$

where S_N represents the concentration of nitrogen in the medium and k_N is the half-saturation constant for nitrogen. The specific growth rate utilized in this study is an expansion of the Monod model.

In addition to the Monod model, the Verhulst model was employed to capture the dynamics of biomass accumulation over time. The Verhulst model is expressed as described in (Abdel-Raouf et al., 2012).

$$X(t) = \frac{X_m X_0 e^{\mu t}}{X_m - X_0 + X_{0e^{\mu t}}} \qquad (3)$$

where x represents the biomass concentration of biofilm, x_m represents the maximum cell concentration that the system can reach in batch, X_0 is the initial concentration of microorganism, t represents time and μ is the specific growth rate of the biofilm. The specific growth rate in the extended Monod model (2) is substituted into the Verhulst model (3) to estimate the consortia growth.

2.4 Mathematical modelling and kinetic expression for nutrient uptake by consortia

The equation representing the Verhulst model was used to precisely explain the nutrient absorption by the consortia (Álvarez-Díaz et al., 2017).

$$S = \frac{\left(\frac{X_0}{Y}+S_0\right)(S_0-S_{na}) - S_{na}\left(\frac{X_0}{Y}+S_0\right)}{(S_0-S_{na}) - \left(S_0-\left(\frac{X_0}{Y}+S_0\right)\right)e^{pt}} \qquad (4)$$

where S is the total nutrient concentration, S_0 represents the initial amount of substrate concentration in the culture medium, S_{na} is the unassimilated substrate concentration and p denotes the specific consortia growth rate and Y is the consortia yield coefficient for the ratio of biomass produced per mass of substrate incorporated as organic or structural which can be calculated using the equation as stated below

$$Y = \left[\left(\frac{X_m - X_0}{S_{b-}S_{na}}\right)\right] \qquad (5)$$

By some transformations to (4) as outlined in the study by Álvarez-Díaz et al., (2017), the equation can be modified to resemble equation (3)

Hence, conclude that p indicates the specific growth rate of consortia, μ and t have the same relation to estimate consortia growth and nutrient uptake by using the Verhulst model. Therefore, the specific growth rate, μ of the extended Monod model in (2) will be used in place of p for nutrient absorption by the consortium.

$$X(t) = \frac{X_m X_0 e^{\mu t}}{X_m - X_0 + X_{0e^{\mu t}}} \qquad (6)$$

2.5 EPS determination and quantification

The consortium culture was centrifuged at 14000×g for 15 min (sigma 2-16KL, Germany). Ethanol was added to the supernatant in a common ratio of 1:3 (supernatant: ethanol), which induces precipitation of the EPS. The supernatant with 95% cold ethanol was vigorously stirred and then kept for 24 h at 4°C to ensure complete EPS precipitation. Subsequently, the precipitates were collected by centrifugation at 14000×g for 20 min and the supernatant was removed (Padmanaban et al., 2015). After ethanol precipitation, the EPS pellet was washed and dehydrated with cold ethanol and acetone to minimize contamination from low molecular weight compounds and salts. The repeated washing is reported to significantly improve EPS purity (Khanal et al., 2017). The recovered EPS was figured out gravimetrically by g/L of culture medium and then made to dry. The dehydrated EPS was weighed for up to 45 days during the culture process.

2.6 Characterization of morphology

The SEM analysis was used to examine the morphological features of the bacterial consortium-associated EPS. The bacterial consortium was then dehydrated using ethanol at different concentrations and the pellet was collected using an ultrafiltration after seven days of growth. The dehydrated pellet was then analysed using SEM to evaluate the formation of biofilm and aggregation of cells via EPS (Jyoti et al., 2024). The same procedure was repeated on the 45th day of growth to observe any changes during the incubation period (Rangaswamy et al., 2020).

2.7 Physiochemical properties of ammonia, nitrite, nitrate, and nitrogen flux

The phenate method was used to measure and record the levels of ammonia, nitrite, and nitrate in the samples in order to assess the efficacy of the nitrification process in the consortium sample that was fed with NH_4Cl (Joseph et al., 2021). The values were measured before feeding, during feeding, and after feeding of NH_4Cl.

2.7.1 Estimation of ammonia

1mL of sample was mixed with 0.4 mL of sodium phenate (1.06 M) and sodium nitroprusside solution (16 mM), followed by the addition of 1 mL of oxidizing reagent, prepared by combining 100 mL of alkaline solution [0.6 M trisodium citrate, 0.25 N sodium hydroxide] with 25 mL of sodium hypochlorite solution (5% w/v). Finally, the volume was made up to 10 mL with double-distilled water.

2.7.2 Estimation of nitrite

The 10 mL of a sample was added with 0.2 mL of sulphanilamide solution (1% (w/v) in 1 N HCl) and 0.2 mL of NED. The reading was taken after 8 min at the absorbance of 543 nm.

2.7.3 Estimation of nitrate

A mixture was prepared by adding 10 mL of the sample, 0.4 mL of buffer reagent (5% w/v in buffer phenol solution in 0.125 N and NaOH 1:1 ratio), 0.2 mL of 0.00465 M hydrazine sulphate, 0.0008 M $CuSO_4$ in a 1:1 ratio and then incubated in the dark for 18-24 h and again added 0.4 mL of acetone, 0.2 mL sulphanilamide, and 0.2 mL 5 mM NED. The reading was measured after 8 min at the absorbance of 543 nm.

2.8 Determination of inorganic nitrogen flux

The inorganic nitrogen fluxes in the consortia sample were calculated using the following equation (Yan et al., 2024).

$$F = \frac{\Delta C. V}{A. \Delta t}$$

where F (mg $m^{-2}d^{-1}$) represents inorganic nitrogen fluxes; V (m^3) is the volume of the flask; A (m^2) is the bottom area of the flask; Δt (d) denotes the incubation duration; and $\Delta C\left(\frac{mg}{l}\right)$ stands the change in the concentrations of ammonia, nitrite, and nitrate before and after incubation.

2.9 DNA extraction

Genomic DNA was isolated from the sediment using the protocol described by (Araya et al., 2003) with slight modifications. The extracted DNA was added with 10 mL of CTAB buffer and tube was vortexed and placed in a shaking incubator for 10 min at 60°C. Subsequently, it was centrifuged at 1500×g for 15 min to separate layers. The supernatant was added with cool Isopropanol and 5M NaCl. Stored at -20°C for overnight. After centrifugation at 1500×g for 15 min, the entire solution was removed from the pellet. 2 mL of 70% ethanol was added to the tube and centrifuged at 1500×g for 2 min. The rest of the ethanol was discarded and dried for 30 min. 10 mM of Tris HCl was added and the collected samples were subsequently stored at -20°C.

2.10 PCR and confirmation of amplicons

PCR was used to screen the exoY gene to detect the presence of EPS in the genomic DNA sample from the consortium bacteria with the forward and reverse primers sequence, 5'-ATGCGTATCGACGGTCATC- 3' and 5'CCGAGGGGGGTGTATCTGACCC-3'. The PCR reaction was carried out at a total volume of 10µL as follows: 5µL of Amp GT PCR master mix (Takara Bio Inc), 0.4µL of both forward and reverse primers each, 3.8µL of DNA template, and made up to 10µl final volume with molecular grade water. The PCR conditions were carried out as an initial denaturation step (at 95°C for 5 min), followed by 37 cycles of repetitions of denaturation (at 95°C for 10 s), annealing at 58°C, extension at 72°C for 1.30 s with the final extension at 72°C for 10 min (Araya et al., 2003). Aliquots of PCR products were analyzed by electrophoresis in 1% (w/v) molecular grade agarose (Sigma-Aldrich, USA) gels containing ethidium bromide (0.5 mg mL^{-1}).

2.11 Orthology of functional genes and Logic circuit of the pathway

The gene circuit was constructed to map regulatory interactions governing EPS biosynthesis in nitrifying consortia, using Boolean logic principles adapted from Boscaino et al. (2019). The EPS functional genes for all consortia-forming bacterial groups in the Kyoto Encyclopedia of Genes and Genomes (KEGG) database were extracted from the datasets. KEGG programming interface information regarding the gene orthology of the bacterial organisms was obtained. The orthology content of each organism was converted into a binary logical content vector denoted by "1" (indicating the presence of the ortholog) and "0" (indicating its absence) among all orthologs found in the KEGG database. Modelling circuits of biological pathways focuses on the active events that lead to activation. Entries are compared in GErel based on the selection of genes in the initial two consecutive reactions.

2.12 Statistical analysis

Statistical analysis was performed to assess the significance of the results. Normality test was assessed by the Shapiro–Wilk. A one-way Analysis of Variance (ANOVA) was performed to identify significant differences ($p \leq 0.05$) in biofilm development.

3. Results

The collected wastewater sample was characterized for a basic understanding of the microbial community. The pH of the domestic wastewater was found to be 7.71, indicating no extreme acidity/alkalinity. The turbidity value for wastewater was 151.0 NTU, which signifies suspended solids, potentially from organic/inorganic pollutants. The electrical conductivity value was 4600 µS/cm**.** Conductivity plays a crucial role in wastewater quality control, as it can predict the degree of mineralization and salinity in the wastewater. TSS (1480 mg/L) and TDS (2200 mg/L) were primarily composed of dissolved solids rather than suspended solids, which may suggest the presence of soluble contaminants like heavy metals. The total solids value of 3882.0 mg/L was below the maximum limit of 500 mg/L. In this study, COD levels were 1200 mg/L, above the usual criteria that indicate excessive oxidizable contaminants. The BOD level was 726 mg/L, which is necessary for the aerobic breakdown of dissolved organic materials over five days.

3.1 Consortia development

The extended Monod and Verhulst models were used to estimate consortia growth on the 45th day in domestic wastewater **(Table 1)**. **Fig. 1** shows consortia growth in wastewater treatment plants, and the maximum cell concentration on the 45th day OD value was 5.39. The sustained increase in OD values throughout the incubation period signifies strong consortia development and maturation, highlighting the importance of long-term culture techniques in studying consortium development. The normality of consortia development by Shapiro-Wilk was 0.92 and statistically significant by ANOVA ($p < 0.0005$).

3.2 Characterization of Consortia

SEM analysis qualitatively revealed structural differences between early (day 7–10) and mature (day 45) consortia, showing increased clustering and EPS embedding over time **(Fig. 2)**. It is recognized that sample preparation involving centrifugation and dehydration can alter ultrastructural features; thus, the images were interpreted only qualitatively. During the early stages, the consortia exhibited a sparse and irregular structure with less complexity in the cell structure (Fig. 2a). In contrast to the 45^{th} day, the consortium growth has significantly increased in complexity, displaying a dense network of clustered cells embedded with a well-developed extracellular matrix and the morphological characteristics of consortia were rod-shaped as expressed in **Fig. 2b and 2c**. SEM analysis of the consortium culture on the initial 10^{th} day showed minimal EPS presence despite the denser EPS matrix interaction among microorganisms **(Fig. 2d)**. By the 45th day, cells exhibited a dense network and superior complexity due to increased EPS formation and well-developed EPS structures **(Fig. 2e and 2f)**. The observed increase in cell aggregation and extracellular matrix formation was consistent with previous SEM studies of wastewater biofilms (Sheng et al., 2010).

3.3 EPS formation

The growth of EPS in the culture medium was gradually increased, enhancing the consortia growth and the maximum EPS production on the 45^{th} day was 2.63 g/L (**Fig. 3).** The normality of EPS production was 0.88, were identified by the Shapiro-Wilk. ANOVA results prove statistically significant, which determines the high production of EPS ($p < 0.05$).

3.3 Substrate utilization and nitrogen flux resembling autotrophic population

The consortia culture was fed with NH_4Cl at an initial concentration of 10 ppm. The amount of ammonia, nitrite, and nitrate was estimated by the phenate method. The nitrogen-resembling consortia culture was fed with the NH_4Cl and the ammonia has been utilised by the AOB population for ammonia oxidation, further transferred for the conversion of nitrite formation, utilised by the NOB population and effectively transferred for the nitrate formation **(Table 2)**. This shows that the nitrogen was reduced drastically, proving that the consortia in the wastewater removed the nitrogen, which proves treating wastewater efficiently. This analysis highlights how autotrophic bacteria in consortia culture utilize substrates, focusing on the contributions of AOB and NOB populations **(Fig. 5)**. The nitrogen substrate was consumed by the AOB and NOB populations via the processes of nitrification to nitration. In contrast to this, the changes in the nitrogen source concentration from the nitrogen flux **(Fig. 4)** in the consortium culture were also estimated for 45 days which typically involves measuring the changes in the concentrations of nitrogen compounds (ammonia, nitrite, and nitrate) in the culture after feeding the culture with NH_4Cl at the same concentration of 10 ppm **(Fig. 5)**. The statistical analysis showed no significant difference ($p > 0.1$). These findings indicate that the optimum condition for nitrogen removal and EPS production was achieved at 10 ppm NH_4Cl, 37°C, and 150 rpm over a 45-day incubation period, under which the consortium removed 80% of ammonia and produced 2.63 g/L of EPS.

3.4 PCR and confirmation of amplicons

The exoY gene primer was used to identify the presence of EPS in the consortia sample and produced a DNA fragment between 200-250 bp when annealed at 55°C. Agarose gel image for the obtained PCR product (In well 1, T_a was 51°C; in well 2, T_a was 52°C; in well 3, T_a was 53°C and in well 4 is NTC followed by a 50bp molecular marker in well 5).

3.5 Construction of logic circuits from the amplified PCR product

PCR amplification and orthology data from the KEGG database identified exoY as the sole amplifiable gene linked to EPS synthesis in the consortium, prompting its selection as the circuit's central node. Binary logic gates were defined as follows: A BUFFER gate represented direct, unconditional activation, where exoY presence (input = 1) leads to the activation of exoL which in turn triggered EPS production (output = 1). AND gates were reserved for hypothetical auxiliary interactions, but no co-activators were amplified, limiting the circuit to a simplified BUFFER architecture. OR gates were omitted due to the absence of redundant EPS genes. The logic circuit, structured around a BUFFER gate **(Fig. 6)**, mapped exoY activation directly to exoL gene which in turn linked to succinoglycan (EPS) biosynthesis (Reuber & Walker, 1993).

4. Discussion

4.1 EPS Production Dynamics and Biofilm Structural Maturation

The increase in EPS yield (2.63 g/L on day 45) occurred in connection with qualitative morphological changes observed in SEM, where the irregular structure of early consortia transitioned to a denser, matrix-embedded network at day 45 **(Fig. 2a–f)**, corroborating the role of EPS in stabilizing microbial aggregates (Shukla et al., 2019). The correlation between EPS accumulation and increased aggregate complexity is consistent with reports from wastewater and biofilm studies (Flemming et al., 2010; Sheng et al., 2010). This aligns with studies emphasizing EPS as a structural scaffold that facilitates cell adhesion and nutrient retention within biofilms (Bhawal et al., 2022; Zhao et al., 2019). The maximum EPS production was 2.63 g/L on the 45th day **(Fig. 3)**, while repeated wash steps were used to minimize interference by salts and small metabolites. The observed trend of EPS accumulation correlates strongly with consortia growth and is consistent with EPS yields reported in wastewater consortia (Prete et al., 2021;Nguyen et al., 2024).

The SEM-derived biofilm architecture corroborates Wang et al. (2023), who linked structural complexity to the choice of substrate. However, further studies are recommended. SEM examination provided comparative evidence of increased extracellular and microbial aggregation over time. SEM does not fully preserve in situ biofilm architecture, the observed rod-shaped morphology and progressive aggregate complexity are consistent with earlier reports on substrate-linked biofilm development (Liu et al., 2023). The rod-shaped morphology is also consistent with taxa such as

Rhizobium spp. (Kaur et al., 2011) and *Pseudomonas* spp., with genomic detection of the exoY gene supporting their role in EPS overproduction. These findings should be interpreted qualitatively and in conjunction with EPS biochemical data, rather than as definitive structural proof. The temporal correlation between biofilm complexity and EPS accumulation underscores the necessity of prolonged incubation (45 days). While previous studies have reported high EPS yields within shorter incubation periods under optimized conditions, such systems often lack long-term stability or reusability. On the other hand, our study's 45-day duration of EPS synthesis suggests potential for biofilm regeneration. This indicates that, beyond initial yield, the consortium offers advantages in terms of durability and cost-effectiveness, making it a promising approach for industrial-scale applications. Future work should focus on evaluating the consortia's regeneration capacity of the EPS-producing biofilm under repeated substrate loading in large-scale operational settings.

The gravimetric quantification of EPS, performed using ethanol precipitation and subsequent washing, revealed a gradual increase, peaking at 2.63 g/L by day 45 **(Fig. 3)**. Due to precipitation of bound solutes, multiple washing steps were included to minimize the artefact. The observed yields are consistent with previous reports on wastewater consortia (1.5–3.0 g/L; More et al., 2014), and higher than pure cultures (0.042 g/L in 96 h; Sellami et al., 2015). This increase was similar to microbial growth phases, with EPS production elevated during exponential growth due to active nutrient assimilation and sustained during late stages due to consortia stability. This long-term stability is consistent with broader trends in environmental remediation, where sustained performance is critical for effective pollutant removal (Waliullah et al., 2023). The observed EPS yield surpasses values reported for monocultures like *Bacillus* sp. 1.67 ± 0.06 g/L (Yin et al., 2022) and *L. plantarum* 0.630 g/L (Zhang et al., 2023), underscoring the advantage of consortia in leveraging metabolic diversity. The integration of ammonium chloride as a nitrogen source likely enhanced autotrophic nitrifier activity, further driving EPS biosynthesis through metabolic synergy between AOB and NOB. This synergy is supported by findings that ammonium loading stimulates the abundance of both nitrifying (*Nitrospira*) and denitrifying genera (*Magnetospirillum*, *Dechloromonas*, *Flavobacterium*), facilitating coupled nitrification–denitrification processes that contribute to biofilm development and nutrient cycling (L. Yan et al., 2019). Moreover, discrepancies in optimal pH (Jyoti et al., 2024) and incubation duration (Sellami et al., 2015) highlight context-dependent variability in EPS production, necessitating strain-specific optimisation.

4.2 Kinetic Modelling of Consortium Growth and Substrate Utilization

The Monod and Verhulst models served as reliable tools for analyzing the growth kinetics of the consortium and its use of nitrogen substrates. Such modelling approaches are widely applied in environmental systems to optimize process efficiency and predict system behavior under varying operational conditions (Islam, Teo, et al., 2025). The Monod-derived maximum specific growth rate

(μ_{max} = 5.39) and half-saturation constant (k_n = 2.69) **(Table 1)** reflect efficient nitrogen assimilation, particularly under high substrate availability (S_n = 10 ppm). The Verhulst model further shows that biomass accumulation, predicting a maximum cell concentration (X_m = 1.63 g/L**)**. The nitrogen flux analysis revealed that AOB oxidized 80% of the initial ammonium (8 ppm), while 42% of nitrite (4.2 ppm) was further metabolized by NOB. The accumulation of residual nitrate (1.6 ppm) suggests the potential for downstream denitrification, indicating that the consortium may support both nitrification and partial denitrification under appropriate conditions, a trait advantageous for wastewater treatment. The performance observed under 10 ppm NH_4Cl and extended incubation suggests that this condition supports both autotrophic nitrifier activity and sustained EPS synthesis. Within the scope of this study, they represent an optimal operational window for enhanced pollutant removal and biofilm development.

4.3 Gene Circuit Engineering and exoY Amplification in EPS Biosynthesis

The exclusive amplification of exoY gene highlights its dominant role in EPS biosynthesis within the consortium. KEGG orthology traces exoY to Rhizobiaceae, suggesting *Rhizobium*-related species, which is known for its symbiotic nitrogen fixation and succinoglycan production which may dominate the consortium (Jones, 2012; Ratib et al., 2018). While *Rhizobium* is not classically autotrophic, its presence could synergize with undetected AOB, as *Rhizobium*-derived EPS may stabilize biofilms, enhancing retention of autotrophic nitrifiers. The observed nitrification efficiency likely arises from such metabolic partnerships, where *Rhizobium*'s heterotrophic activity complements autotrophic ammonia oxidation by AOB. The BUFFER gate's simplicity reflects the consortium's reliance on exoY driven EPS synthesis. The exploration of genetic regulation in microbial systems aligns with ongoing developments in environmental biotechnology aimed at enhancing treatment precision and adaptability (Hasan et al., 2023). Moreover, the consortium's higher EPS yield (2.63 g/L) suggests that using EPS producing bacterial consortium in water treatment plants, particularly by over expressing the exoY gene is promising when compared to single strains (2.45 g/L in *Serratia sp.1*) used in previous studies with similar conditions (Bezawada et al., 2013). Future work could integrate inducible promoters to further enhance EPS titers.

4.4 Implications for Wastewater Treatment and Biotechnological Applications

The consortium's ability to reduce ammonium from 10 ppm to 2 ppm over 45 days demonstrates its efficacy in nitrogen removal, a critical metric for wastewater treatment. However, enhancing exoY gene expression might reduce this time frame further. The sequential oxidation of ammonia to nitrate, coupled with partial denitrification, could be a sustainable alternative to traditional methods. The EPS matrix's metal-binding capacity, attributed to uronic acids and sulphates (Freire-Nordi et al., 2005), positions the consortium as a candidate for bioremediation of heavy metal-laden effluents. This integrated approach reflects the broader movement toward multifunctional treatment

systems that combine pollutant removal with resource recovery (Awual, 2019; Islam et al., 2024). This opens the door for further research in the field of bioremediation.

5. Conclusion

This study establishes a novel integrative framework that combines kinetic modelling, biofilm structural analysis, and synthetic gene circuit design to optimize EPS production in nitrifying bacterial consortia for wastewater treatment. Key innovations include the dual application of Monod and Verhulst models to predict consortium growth (OD_{590} = 5.39) and substrate utilization under controlled nitrogen flux (10 ppm NH_4Cl), resulting in a maximum EPS yield of 2.63 g/L by day 45. The construction of a BUFFER-gate logic gene circuit, based on the presence of the exoY gene, provided a conceptual model for EPS biosynthesis regulation within the consortium. SEM imaging confirmed progressive biofilm maturation, with increased EPS accumulation correlating with structural complexity. Functionally, the consortium achieved 80% ammonia oxidation by autotrophic populations, with subsequent nitrite and nitrate transformations. Compared to monoculture systems, which often exhibit lower EPS yields and reduced metabolic versatility, the consortium demonstrated enhanced biopolymer production and pollutant removal. This highlights the advantage of metabolic cooperation in mixed microbial systems.

In conclusion, this work advances the rational engineering of microbial consortia by integrating kinetic and genetic modelling approaches. Future research should explore inducible exoY expression systems and evaluate the consortium's performance in field-scale applications, particularly for heavy metal remediation. Additionally, implementing comprehensive microbial community analysis techniques, such as 16S rRNA gene amplicon sequencing for taxonomic profiling, and metagenomics or meta transcriptomics for assessing functional potential and active gene expression, would enable confirmation of key microbial groups (e.g., AOB, NOB, Rhizobium) and provide insights into metabolic interdependencies. These approaches could support the design of more stable, resilient, and efficient consortia.

Acknowledgment

The authors are grateful to the Department of Science and Technology (DST), Government of India, New Delhi, India for the financial support of the research facility at PSG College of Arts & Science College, Coimbatore, India as part of Fund for the Improvement of S & T Infrastructure (DST – FIST).

Conflict of interest

The authors declare that they have no conflict of interest.

Informed consent statement

Not applicable.

Consent to publish

All authors approved the manuscript and gave their consent for submission and publication.

Data availability statement

There is no research related data stored in publicly available repositories, and the data will be made available on request.

Declaration of Interest Statement

The authors declare that they have no known competing financial interests or personal relationships that could have appeared to influence the work reported in this paper.

Author contribution

Indhuja Sakthivel: Methodology, Validation, Formal analysis, Writing - Original Draft. **Boobal Rangaswamy:** Conceptualization, Methodology, Validation, Formal analysis, Visualization, Data curation, Writing – original draft, Writing –review & editing, Supervision, Investigation. **Bharathkumar Rajagopal:** Writing - Original Draft, Writing - Review & Editing. **Lathika Shanmugam:** Data Curation, Visualization, Writing - Original Draft, Writing - Review & Editing.

Declaration of Competing Interest

The authors declare that they have no known competing financial interests or personal relationships that could have appeared to influence the work reported in this paper.

Funding

This research did not receive any specific grant from funding agencies in the public, commercial, or not-for-profit sectors.

References

1. Abdel-Raouf, N., Al-Homaidan, A. A., & Ibraheem, I. B. M. (2012). Microalgae and wastewater treatment. *Saudi Journal of Biological Sciences*, *19*(3), 257–275. https://doi.org/10.1016/j.sjbs.2012.04.005
2. Álvarez-Díaz, P. D., Ruiz, J., Arbib, Z., Barragán, J., Garrido-Pérez, M. C., & Perales, J. A. (2017). Freshwater microalgae selection for simultaneous wastewater nutrient removal and lipid production. *Algal Research*, *24*, 477–485. https://doi.org/10.1016/j.algal.2017.02.006
3. Araya, R., Tani, K., Takagi, T., Yamaguchi, N., & Nasu, M. (2003). Bacterial activity and community composition in stream water and biofilm from an urban river determined by fluorescent in situ hybridization and DGGE analysis. *FEMS Microbiology Ecology*, *43*(1), 111–119. https://doi.org/10.1111/j.1574-6941.2003.tb01050.x
4. Awual, M. R. (2019). An efficient composite material for selective lead(II) monitoring and removal from wastewater. *Journal of Environmental Chemical Engineering*, *7*(3), 103087. https://doi.org/10.1016/j.jece.2019.103087
5. Awual, M. R., Hasan, M. M., Islam, A., Asiri, A. M., & Rahman, M. M. (2020). Optimization of an innovative composited material for effective monitoring and removal of cobalt(II) from wastewater. *Journal of Molecular Liquids*, *298*, 112035. https://doi.org/10.1016/j.molliq.2019.112035
6. Awual, M. R., Hasan, M. M., Islam, A., Rahman, M. M., Asiri, A. M., Khaleque, M. A., & Sheikh, M. C. (2019). Introducing an amine functionalized novel conjugate material for toxic nitrite detection and adsorption from wastewater. *Journal of Cleaner Production*, *228*, 778–785. https://doi.org/10.1016/j.jclepro.2019.04.280
7. Awual, M. R., Hasan, M. M., Khaleque, M. A., & Sheikh, M. C. (2016). Treatment of copper(II) containing wastewater by a newly developed ligand based facial conjugate materials. *Chemical Engineering Journal*, *288*, 368–376. https://doi.org/10.1016/j.cej.2015.11.108
8. Awual, M. R., Hasan, M. M., Rahman, M. M., & Asiri, A. M. (2019). Novel composite material for selective copper(II) detection and removal from aqueous media. *Journal of Molecular Liquids*, *283*, 772–780. https://doi.org/10.1016/j.molliq.2019.03.141
9. Bezawada, J., Hoang, N. V., More, T. T., Yan, S., Tyagi, N., Tyagi, R. D., & Surampalli, R. Y. (2013). Production of extracellular polymeric substances (EPS) by Serratia sp.1 using wastewater sludge as raw material and flocculation activity of the EPS produced. *JOURNAL OF ENVIRONMENTAL MANAGEMENT*, *128*, 83–91. https://doi.org/10.1016/j.jenvman.2013.04.039
10. Bhattacharya, M., Guchhait, S., Biswas, D., & Singh, R. (2019). Evaluation of a microbial consortium for crude oil spill bioremediation and its potential uses in enhanced oil recovery.

Biocatalysis and Agricultural Biotechnology, *18*, 101034. https://doi.org/10.1016/j.bcab.2019.101034

11. Bhawal, S., Kumari, A., Kapila, S., & Kapila, R. (2022). Biofunctional Attributes of Surface Layer Protein and Cell-Bound Exopolysaccharide from Probiotic Limosilactobacillus fermentum (MTCC 5898). *Probiotics and Antimicrobial Proteins*, *14*(2), 360–371. https://doi.org/10.1007/s12602-021-09891-4
12. Boscaino, V., Fiannaca, A., La Paglia, L., La Rosa, M., Rizzo, R., & Urso, A. (2019). MiRNA therapeutics based on logic circuits of biological pathways. *BMC Bioinformatics*, *20*(S9), 344. https://doi.org/10.1186/s12859-019-2881-7
13. Cai, M., Ng, S.-K., Lim, C. K., Lu, H., Jia, Y., & Lee, P. K. H. (2018). Physiological and Metagenomic Characterizations of the Synergistic Relationships between Ammonia- and Nitrite-Oxidizing Bacteria in Freshwater Nitrification. *Frontiers in Microbiology*, *9*, 280. https://doi.org/10.3389/fmicb.2018.00280
14. Chen, C., Ali, A., Su, J., Wang, Y., Huang, T., & Gao, J. (2021). Pseudomonas stutzeri GF2 augmented the denitrification of low carbon to nitrogen ratio: Possibility for sewage wastewater treatment. *Bioresource Technology*, *333*, 125169. https://doi.org/10.1016/j.biortech.2021.125169
15. Del Nery, V., Damianovic, M. H. Z., Moura, R. B., Pozzi, E., Pires, E. C., & Foresti, E. (2016). Poultry slaughterhouse wastewater treatment plant for high quality effluent. *Water Science and Technology*, *73*(2), 309–316. https://doi.org/10.2166/wst.2015.494
16. Dmitry, D., Stanislav, D., Evgenya, P., & Mikhail, T. (2015). Optimization of the process of cultivation of microalgae chlorella vulgaris biomass with high lipid content for biofuel production. *Chemical Engineering Transactions*, *43*, 361–366. https://doi.org/10.3303/CET1543061
17. Flemming, H.-C., & Wingender, J. (2010). The biofilm matrix. *Nature Reviews Microbiology*, *8*(9), 623–633. doi: 10.1038/nrmicro2415
18. Freire-Nordi, C. S., Vieira, A. A. H., & Nascimento, O. R. (2005). The metal binding capacity of Anabaena spiroides extracellular polysaccharide: an EPR study. *Process Biochemistry*, *40*(6), 2215–2224. https://doi.org/10.1016/j.procbio.2004.09.003
19. Guibaud, G., Bhatia, D., d'Abzac, P., Bourven, I., Bordas, F., Van Hullebusch, E. D., & Lens, P. N. L. (2012). Cd(II) and Pb(II) sorption by extracellular polymeric substances (EPS) extracted from anaerobic granular biofilms: Evidence of a pH sorption-edge. *Journal of the Taiwan Institute of Chemical Engineers*, *43*(3), 444–449. https://doi.org/10.1016/j.jtice.2011.12.007
20. Hamzah, A., Phan, C.-W., Abu Bakar, N. F., & Wong, K.-K. (2013). Biodegradation of Crude Oil by Constructed Bacterial Consortia and the Constituent Single Bacteria Isolated From

Malaysia. *Bioremediation Journal*, *17*(1), 1–10. https://doi.org/10.1080/10889868.2012.731447

21. Hasan, M. M., Salman, M. S., Hasan, M. N., Rehan, A. I., Awual, M. E., Rasee, A. I., Waliullah, R. M., Hossain, M. S., Kubra, K. T., Sheikh, M. C., Khaleque, M. A., Marwani, H. M., Islam, A., & Awual, M. R. (2023). Facial conjugate adsorbent for sustainable Pb(II) ion monitoring and removal from contaminated water. *Colloids and Surfaces A: Physicochemical and Engineering Aspects*, *673*, 131794. https://doi.org/10.1016/j.colsurfa.2023.131794
22. Hasan, M. N., Salman, M. S., Islam, A., Znad, H., & Hasan, M. M. (2021). Sustainable composite sensor material for optical cadmium(II) monitoring and capturing from wastewater. *Microchemical Journal*, *161*, 105800. https://doi.org/10.1016/j.microc.2020.105800
23. He, Y., Liu, Y., Li, X., Zhu, T., & Liu, Y. (2023). Unveiling the roles of biofilm in reducing N2O emission in a nitrifying integrated fixed-film activated sludge (IFAS) system. *Water Research*, *243*, 120326. https://doi.org/10.1016/j.watres.2023.120326
24. Heilmann, C., & Götz, F. (2009). Cell–Cell Communication and Biofilm Formation in Gram-Positive Bacteria. In R. Krämer & K. Jung (Eds.), *Bacterial Signaling* (1 ed., pp. 7–22). Wiley.
25. Hwi Jeong, D., & Min Lee, J. (2013). Integrating Flux Balance Analysis into Microalgae Growth Kinetics for Dynamic Simulation. *IFAC Proceedings Volumes*, *46*(32), 295–300. https://doi.org/10.3182/20131218-3-in-2045.00080
26. Islam, A., Islam, T., Mahmud, H., Raihan, O., Islam, M. S., Marwani, H. M., Rahman, M. M., Asiri, A. M., Hasan, M. M., Hasan, M. N., Salman, M. S., Kubra, K. T., Shenashen, M. A., Sheikh, M. C., & Awual, M. R. (2024). Accelerating the green hydrogen revolution: A comprehensive analysis of technological advancements and policy interventions. *International Journal of Hydrogen Energy*, *67*, 458–486. https://doi.org/10.1016/j.ijhydene.2024.04.142
27. Islam, A., Malek, A., Islam, M. T., Nipa, F. Y., Raihan, O., Mahmud, H., Uddin, M. E., Ibrahim, M. L., Abdulkareem-Alsultan, G., Mondal, A. H., Hasan, M. M., Salman, M. S., Kubra, K. T., Hasan, M. N., Sheikh, M. C., Uchida, T., Rasee, A. I., Rehan, A. I., Awual, M. E.,…Awual, M. R. (2025). Next frontier in photocatalytic hydrogen production through CdS heterojunctions. *International Journal of Hydrogen Energy*, *101*, 173–211. https://doi.org/10.1016/j.ijhydene.2024.12.300
28. Islam, A., Teo, S. H., Islam, M. T., Mondal, A. H., Mahmud, H., Ahmed, S., Ibrahim, M., Taufiq-Yap, Y. H., G, A.-A., Hossain, M. L., Sheikh, M. C., Rasee, A. I., Rehan, A. I., Waliullah, R. M., Awual, M. E., Hasan, M. M., Hossain, M. S., Kubra, K. T., Salman, M. S.,…Awual, M. R. (2025). Harnessing visible light for sustainable biodiesel production with Ni/Si/MgO photocatalyst. *Renewable and Sustainable Energy Reviews*, *208*, 115033. https://doi.org/10.1016/j.rser.2024.115033

29. Janczarek, M. (2011). Environmental Signals and Regulatory Pathways That Influence Exopolysaccharide Production in Rhizobia. *International Journal of Molecular Sciences*, *12*(11), 7898–7933. https://doi.org/10.3390/ijms12117898
30. Jones, K. M. (2012). Increased Production of the Exopolysaccharide Succinoglycan Enhances Sinorhizobium meliloti 1021 Symbiosis with the Host Plant Medicago truncatula. *Journal of Bacteriology*, *194*(16), 4322–4331. https://doi.org/10.1128/JB.00751-12
31. Joseph, V., Chellappan, G., Aparajitha, S., Ramya, R. N., Vrinda, S., Rejish Kumar, V. J., & Bright Singh, I. S. (2021). Molecular characterization of bacteria and archaea in a bioaugmented zero-water exchange shrimp pond. *SN Applied Sciences*, *3*(4), 458. https://doi.org/10.1007/s42452-021-04392-z
32. Jyoti, K., Soni, K., & Chandra, R. (2024). Optimization of the production of Exopolysaccharide (EPS) from biofilm-forming bacterial consortium using different parameters. *The Microbe*, *4*, 100117. https://doi.org/10.1016/j.microb.2024.100117
33. Kaur, J., Verma, M., & Lal, R. (2011). Rhizobium rosettiformans sp. nov., isolated from a hexachlorocyclohexane dump site, and reclassification of Blastobacter aggregatus Hirsch and Müller 1986 as Rhizobium aggregatum comb. nov. *International Journal of Systematic and Evolutionary Microbiology*, *61*(5), 1218–1225. https://doi.org/10.1099/ijs.0.017491-0
34. Khanal, S. N., & Lucey, John. A. (2017). Evaluation of the yield, molar mass of exopolysaccharides, and rheological properties of gels formed during fermentation of milk by Streptococcus thermophilus strains St-143 and ST-10255y. *Journal of Dairy Science*, *100*(9), 6906–6917. doi: 10.3168/jds.2017-12835
35. Kreft, J. U., & Wimpenny, J. W. (2001). Effect of EPS on biofilm structure and function as revealed by an individual-based model of biofilm growth. *Water Science and Technology*, *43*(6), 135–135. https://doi.org/10.2166/wst.2001.0358
36. Lezia, A., Miano, A., & Hasty, J. (2022). Synthetic Gene Circuits: Design, Implement, and Apply. *Proceedings of the IEEE*, *110*(5), 613–630. https://doi.org/10.1109/JPROC.2021.3134169
37. Li, X., Du, R., Peng, Y., Zhang, Q., & Wang, J. (2020). Characteristics of sludge granulation and EPS production in development of stable partial nitrification. *Bioresource Technology*, *303*, 122937. https://doi.org/10.1016/j.biortech.2020.122937
38. Liu, Y. (2006). A simple thermodynamic approach for derivation of a general Monod equation for microbial growth. *Biochemical Engineering Journal*, *31*(1), 102–105. https://doi.org/10.1016/j.bej.2006.05.022
39. Liu, S., Liu, B., Zhu, Y., Qiu, Y., & Li, B. (2023). The Spatial–Temporal Effects of Bacterial Growth Substrates on Antibiotic Resistance Gene Spread in the Biofilm. *Antibiotics*, *12*(7), 1154. doi: 10.3390/antibiotics12071154

40. Marques, R., Von Stosch, M., Portela, R. M. C., Torres, C. A. V., Antunes, S., Freitas, F., Reis, M. A. M., & Oliveira, R. (2017). Hybrid modeling of microbial exopolysaccharide (EPS) production: The case of Enterobacter A47. *Journal of Biotechnology*, *246*, 61–70. https://doi.org/10.1016/j.jbiotec.2017.01.017
41. More, T. T., Yadav, J. S. S., Yan, S., Tyagi, R. D., & Surampalli, R. Y. (2014). Extracellular polymeric substances of bacteria and their potential environmental applications. *Journal of Environmental Management*, *144*, 1–25. doi: 10.1016/j.jenvman.2014.05.010
42. Nguyen, H.-T., Pham, T.-T., Nguyen, P.-T., Le-Buanec, H., Rabetafika, H. N., & Razafindralambo, H. L. (2024). Advances in Microbial Exopolysaccharides: Present and Future Applications. *Biomolecules*, *14*(9), 1162. doi: 10.3390/biom14091162
43. Padmanaban, S., Balaji, N., Muthukumaran, C., & Tamilarasan, K. (2015). Statistical optimization of process parameters for exopolysaccharide production by Aureobasidium pullulans using sweet potato based medium. *3 Biotech*, *5*(6), 1067–1073. https://doi.org/10.1007/s13205-015-0308-3
44. Plattes, M., & Lahore, H. M. F. (2023). Perspectives on the Monod model in biological wastewater treatment. *Journal of Chemical Technology & Biotechnology*, *98*(4), 833–837. https://doi.org/10.1002/jctb.7291
45. Prete, R., Alam, M. K., Perpetuini, G., Perla, C., Pittia, P., & Corsetti, A. (2021). Lactic Acid Bacteria Exopolysaccharides Producers: A Sustainable Tool for Functional Foods. *Foods*, *10*(7), 1653. doi: 10.3390/foods10071653
46. Rangaswamy, B., Ramankutty Nair, R., Achuthan, C., & Isaac Sarojini, B. S. (2020). Computational analysis of successional changes in the microbial population and community diversity of the immobilized marine nitrifying bacterial consortium in a nitrifying packed bed bioreactor. *3 Biotech*, *10*(12), 524. https://doi.org/10.1007/s13205-020-02510-z
47. Ratib, N. R., Sabio, E. Y., Mendoza, C., Barnett, M. J., Clover, S. B., Ortega, J. A., Dela Cruz, F. M., Balderas, D., White, H., Long, S. R., & Chen, E. J. (2018). Genome-wide identification of genes directly regulated by ChvI and a consensus sequence for ChvI binding in *Sinorhizobium meliloti*. *Molecular Microbiology*, *110*(4), 596–615. doi: 10.1111/mmi.14119
48. Rehan, A. I., Rasee, A. I., Awual, M. E., Waliullah, R. M., Hossain, M. S., Kubra, K. T., Salman, M. S., Hasan, M. M., Hasan, M. N., Sheikh, M. C., Marwani, H. M., Khaleque, M. A., Islam, A., & Awual, M. R. (2023). Improving toxic dye removal and remediation using novel nanocomposite fibrous adsorbent. *Colloids and Surfaces A: Physicochemical and Engineering Aspects*, *673*, 131859. https://doi.org/10.1016/j.colsurfa.2023.131859
49. Reuber, T. L., & Walker, G. C. (1993). Biosynthesis of succinoglycan, a symbiotically important exopolysaccharide of Rhizobium meliloti. *Cell*, *74*(2), 269–280. https://doi.org/10.1016/0092-8674(93)90418-P

50. Ruiz, J., Arbib, Z., Álvarez-Díaz, P. D., Garrido-Pérez, C., Barragán, J., & Perales, J. A. (2013). Photobiotreatment model (PhBT): a kinetic model for microalgae biomass growth and nutrient removal in wastewater. *Environmental Technology*, *34*(8), 979–991. https://doi.org/10.1080/09593330.2012.724451

51. Sadiq, U. A. F. M., Yow, M. E., & Jamaian, S. S. (2018). The Extended Monod Model for Microalgae Growth and Nutrient Uptake in Different Wastewaters. *International Journal of Engineering & Technology*, *7*(4.30), 200–204. https://doi.org/10.14419/ijet.v7i4.30.22120

52. Sellami, M., Oszako, T., Miled, N., & Ben Rebah, F. (2015). Industrial wastewater as raw material for exopolysaccharide production by Rhizobium leguminosarum. *Brazilian Journal of Microbiology*, *46*(2), 407–413. https://doi.org/10.1590/S1517-838246220140153

53. Sheng, G.-P., Yu, H.-Q., & Li, X.-Y. (2010). Extracellular polymeric substances (EPS) of microbial aggregates in biological wastewater treatment systems: A review. *Biotechnology Advances*, *28*(6), 882–894. https://doi.org/10.1016/j.biotechadv.2010.08.001

54. Shukla, A., Mehta, K., Parmar, J., Pandya, J., & Saraf, M. (2019). Depicting the exemplary knowledge of microbial exopolysaccharides in a nutshell. *European Polymer Journal*, *119*, 298–310. https://doi.org/10.1016/j.eurpolymj.2019.07.044

55. Smith, L. H., Kitanidis, P. K., & McCarty, P. L. (1997). Numerical modeling and uncertainties in rate coefficients for methane utilization and TCE cometabolism by a methane-oxidizing mixed culture. *Biotechnology and Bioengineering*, *53*(3), 320–331. https://doi.org/10.1002/(SICI)1097-0290(19970205)53:3<320::AID-BIT11>3.0.CO;2-O

56. Song, T., Zhang, X., Li, J., Wu, X., Feng, H., & Dong, W. (2021). A review of research progress of heterotrophic nitrification and aerobic denitrification microorganisms (HNADMs). *Science of The Total Environment*, *801*, 149319. https://doi.org/10.1016/j.scitotenv.2021.149319

57. Song, W., Lee, L. Y., You, H., Shi, X., & Ng, H. Y. (2020). Microbial community succession and its correlation with reactor performance in a sponge membrane bioreactor coupled with fiber-bundle anoxic bio-filter for treating saline mariculture wastewater. *Bioresource Technology*, *295*, 122284. https://doi.org/10.1016/j.biortech.2019.122284

58. Vajda, A. M., Barber, L. B., Gray, J. L., Lopez, E. M., Bolden, A. M., Schoenfuss, H. L., & Norris, D. O. (2011). Demasculinization of male fish by wastewater treatment plant effluent. *Aquatic Toxicology*, *103*(3-4), 213–221. https://doi.org/10.1016/j.aquatox.2011.02.007

59. Waliullah, R. M., Rehan, A. I., Awual, M. E., Rasee, A. I., Sheikh, M. C., Salman, M. S., Hossain, M. S., Hasan, M. M., Kubra, K. T., Hasan, M. N., Marwani, H. M., Islam, A., Rahman, M. M., Khaleque, M. A., & Awual, M. R. (2023). Optimization of toxic dye removal from contaminated water using chitosan-grafted novel nanocomposite adsorbent. *Journal of Molecular Liquids*, *388*, 122763. https://doi.org/10.1016/j.molliq.2023.122763

60. Wang, K., Wang, Z., Ding, Y., Yu, Y., Wang, Y., Geng, Y., Li, Y., & Wen, X. (2023). Optimization of Heterotrophic Culture Conditions for the Algae Graesiella emersonii WBG-1 to Produce Proteins. *Plants*, *12*(12), 2255. https://doi.org/10.3390/plants12122255

61. Wang, Z., Zheng, Y., Guo, J., Lai, Z., Liu, J., Li, N., Li, Z., Gao, M., Qiao, X., Yang, Y., Zhang, H., An, L., & Xu, K. (2025). Recent advance on the production of microbial exopolysaccharide from waste materials. *Bioprocess Biosyst Eng*, *48*(8), 1239–1254. https://doi.org/10.1007/s00449-025-03169-7

62. Xia, S., Song, Z., Jeyakumar, P., Shaheen, S. M., Rinklebe, J., Ok, Y. S., Bolan, N., & Wang, H. (2019). A critical review on bioremediation technologies for Cr(VI)-contaminated soils and wastewater. *Critical Reviews in Environmental Science and Technology*, *49*(12), 1027–1078. https://doi.org/10.1080/10643389.2018.1564526

63. Yan, L., Mu, X., Han, B., Zhang, S., Qiu, C., & Ohore, O. E. (2019). Ammonium loading disturbed the microbial food webs in biofilms attached to submersed macrophyte Vallisneria natans. *Science of The Total Environment*, *659*, 691–698. https://doi.org/10.1016/j.scitotenv.2018.12.423

64. Yan, Y., Zhou, J., Du, C., Yang, Q., Huang, J., Wang, Z., Xu, J., & Zhang, M. (2024). Relationship between Nitrogen Dynamics and Key Microbial Nitrogen-Cycling Genes in an Intensive Freshwater Aquaculture Pond. *Microorganisms*, *12*(2), 266. https://doi.org/10.3390/microorganisms12020266

65. Yin, R., Cheng, J., Wang, J., Li, P., & Lin, J. (2022). Treatment of Pseudomonas aeruginosa infectious biofilms: Challenges and strategies. In Frontiers in Microbiology (Vol. 13). Frontiers Media S.A. doi: 10.3389/fmicb.2022.955286

66. Youssef, H. H., Hamza, M. A., Fayez, M., Mourad, E. F., Saleh, M. Y., Sarhan, M. S., Suker, R. M., Eltahlawy, A. A., Nemr, R. A., El-Tahan, M., Ruppel, S., & Hegazi, N. A. (2016). Plant-based culture media: Efficiently support culturing rhizobacteria and correctly mirror their in-situ diversity. *Journal of Advanced Research*, *7*(2), 305–316. https://doi.org/10.1016/j.jare.2015.07.005

67. Yuan, D., Wang, Y., & Qian, X. (2017). Variations of internal structure and moisture distribution in activated sludge with stratified extracellular polymeric substances extraction. *International Biodeterioration & Biodegradation*, *116*, 1–9. https://doi.org/10.1016/j.ibiod.2016.09.012

68. Zhang, R., Zhou, Z., Ma, Y., Du, K., Sun, M., Zhang, H., Tu, H., Jiang, X., Lu, J., Tu, L., Niu, Y., & Chen, P. (2023). Production of the exopolysaccharide from Lactiplantibacillus plantarum YT013 under different growth conditions: optimum parameters and mathematical analysis. *International Journal of Food Properties*, *26*(1), 1941–1952. https://doi.org/10.1080/10942912.2023.2239518

69. Zhao, J., Liu, S., Liu, N., Zhang, H., Zhou, Q., & Ge, F. (2019). Accelerated productions and physicochemical characterizations of different extracellular polymeric substances from Chlorella vulgaris with nano-ZnO. *Science of The Total Environment*, *658*, 582–589. https://doi.org/10.1016/j.scitotenv.2018.12.019

Figure Caption

Fig. 1 Growth of consortia over 45 days of incubation

Fig. 2 (a) SEM observation on the initial seven days growth of biofilm formation. **(b)** and **(c)** SEM observation on 45 days of growth of biofilm formation. **(d)** SEM observation on the initial seven days of the production of EPS formation. **(e)** and **(f)** SEM observation on the 45-day formation of EPS production.

Fig. 3 Production of EPS enhanced in biofilm over 45 days of incubation

Fig. 4 Nitrogen flux

Fig. 5 Consortia culture fed with NH_4Cl at an initial concentration of 10 ppm. **b.** 8ppm($avg.$) of ammonia utilised by the AOB population for ammonia oxidation. **c.** unassimilated substrate in the consortia culture of value 2ppm($avg.$) **d.** 5ppm ($avg.$) of ammonia transferred for the conversion of nitrite formation. **e.** amount of ammonia utilised by the NOB population for the nitrite oxidation (4.2ppm ($avg.$)). **f.** 0.8ppm ($avg.$) of unutilised nitrite by the bacteria. **g.** 4ppm ($avg.$) of nitrite transformed for the formation of nitrate **h.** 1.6ppm ($avg.$) of nitrate utilised by the bacteria and **i.** remaining 2.4ppm entering into the denitrification process for further metabolism

Fig. 6 KEGG pathway logic modelling

Table 1

Parameters derived for the kinetics of consortia growth and substrate utilisation

Parameters	Values obtained
μ_{max}	5.390
k_N	2.690
S_N	10
X_0	0.42
X_m	1.630

Table 2

Substrate utilization rate quantified based on utilized, unutilized and residues of substrate in the culture

S. No.	Initial fed rate	Substrate utilized	Substrate residues	Presence of a bacterial population
1	10ppm	8ppm	2ppm	Ammonia oxidation
2	5ppm	4.2ppm	0.8ppm	Nitrite oxidation
3	4ppm	1.6ppm	2.4ppm	Nitrate oxidation

Conflict of interest

The authors declare that they have no conflict of interest.

Informed consent statement

Not applicable.

Consent to publish

All authors approved the manuscript and gave their consent for submission and publication.

Data availability statement

There is no research related data stored in publicly available repositories, and the data will be made available on request.

Declaration of Interest Statement

The authors declare that they have no known competing financial interests or personal relationships that could have appeared to influence the work reported in this paper.

Graphical abstract

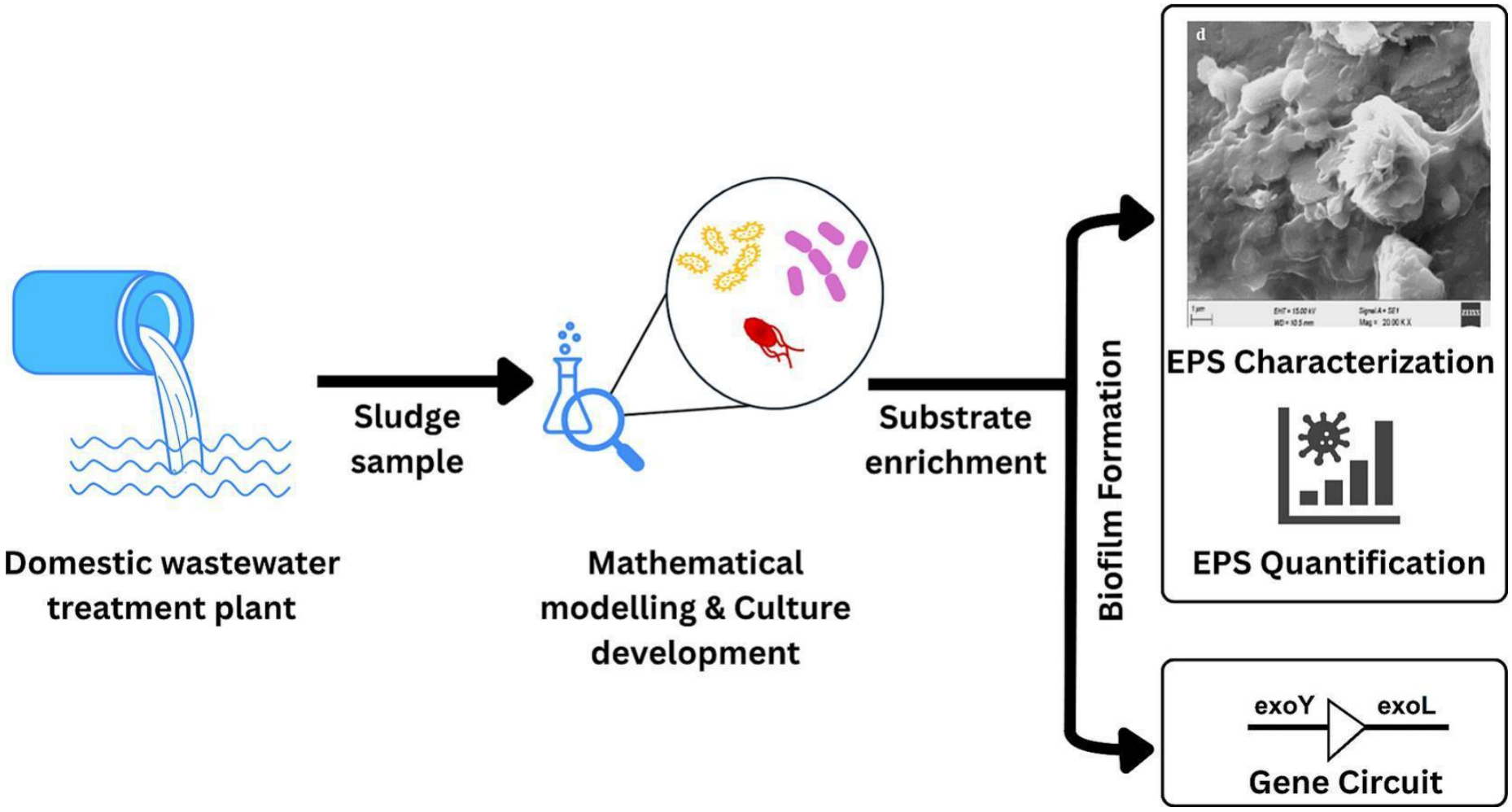

Graphics Abstract

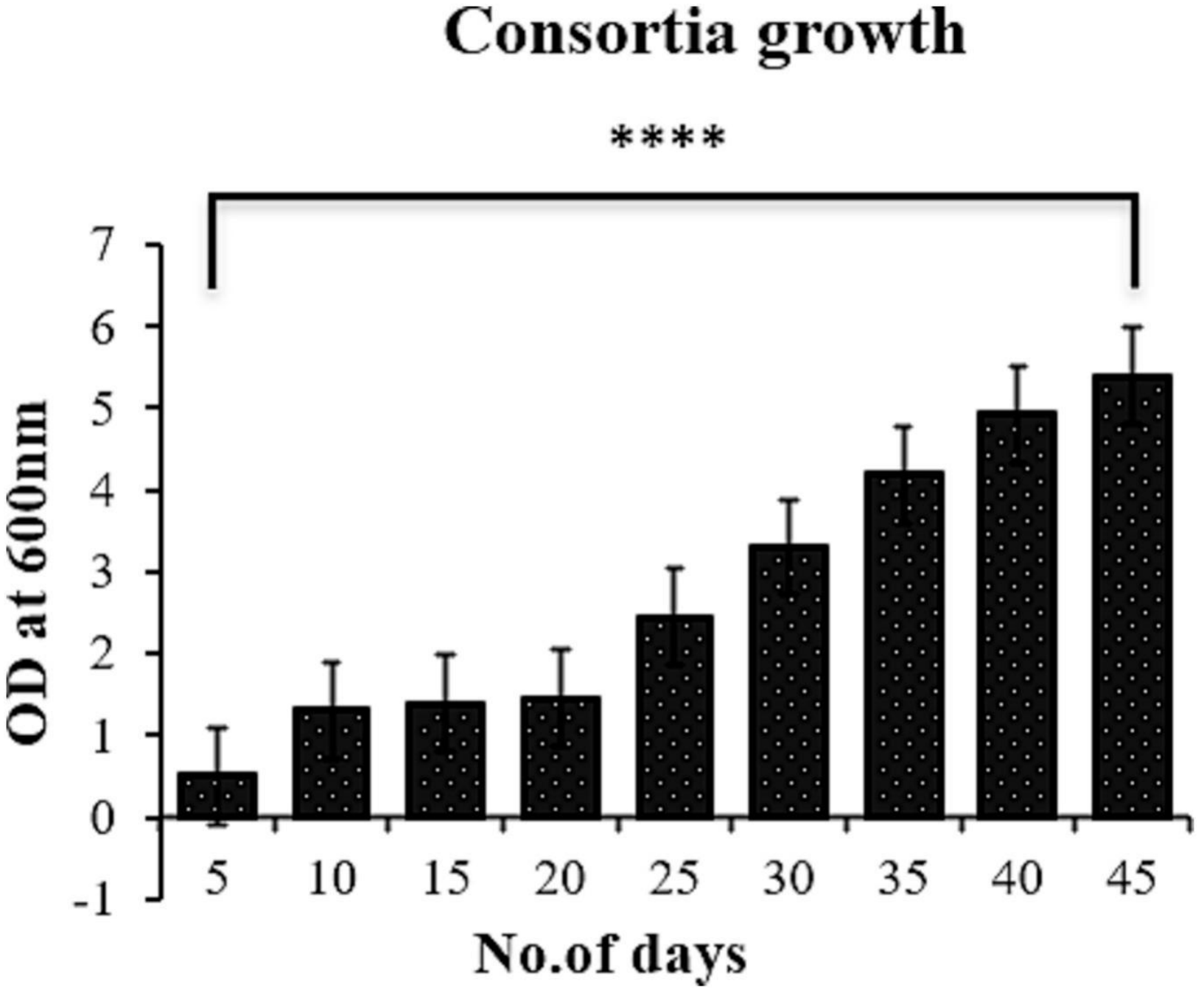
Consortia growth
****
OD at 600nm
7
6
5
4
3
2
1
0
-1
5
10
15
20
25
30
35
40
45
No.of days

Figure 1

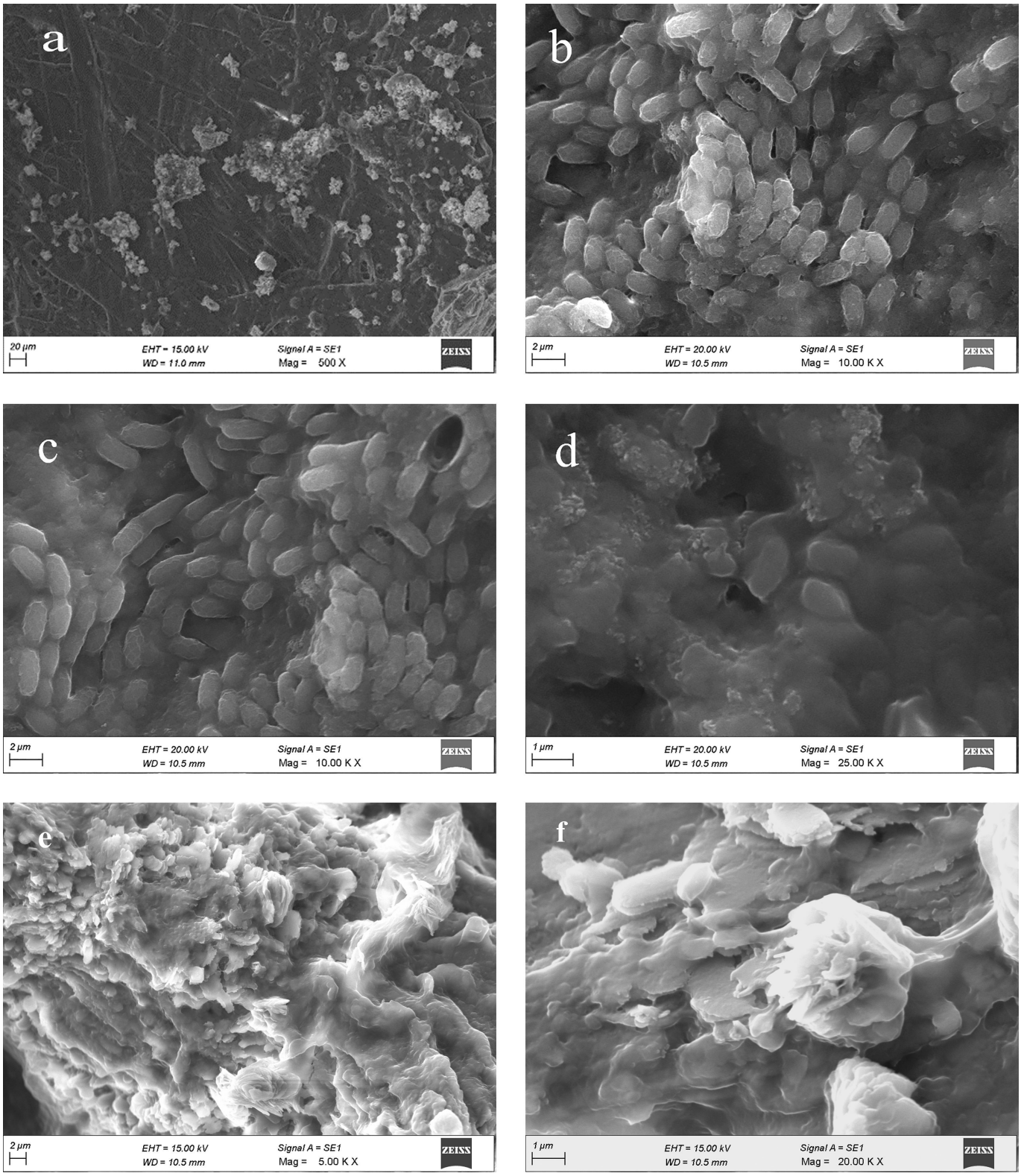
a
20 µm
EHT = 15.00 kV
WD = 11.0 mm
Signal A = SE1
Mag = 500 X
ZEISS
b
2 µm
EHT = 20.00 kV
WD = 10.5 mm
Signal A = SE1
Mag = 10.00 K X
ZEISS
c
2 µm
EHT = 20.00 kV
WD = 10.5 mm
Signal A = SE1
Mag = 10.00 K X
ZEISS
d
1 µm
EHT = 20.00 kV
WD = 10.5 mm
Signal A = SE1
Mag = 25.00 K X
ZEISS
e
2 µm
EHT = 15.00 kV
WD = 10.5 mm
Signal A = SE1
Mag = 5.00 K X
ZEISS
f
1 µm
EHT = 15.00 kV
WD = 10.5 mm
Signal A = SE1
Mag = 20.00 K X
ZEISS

Figure 2

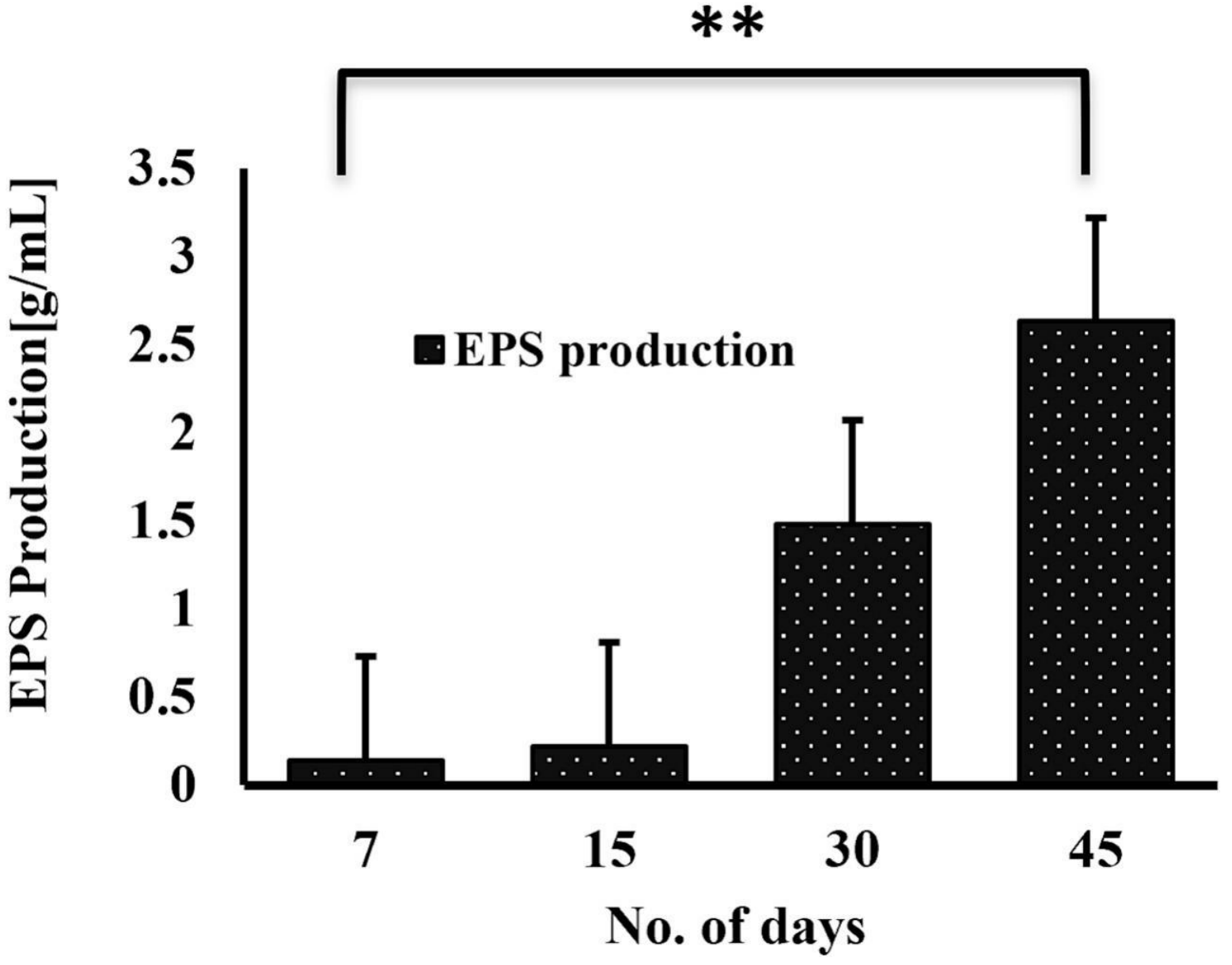
**
EPS Production[g/mL]
3.5
3
2.5
2
1.5
1
0.5
0
EPS production
7
15
30
45
No. of days

Figure 3

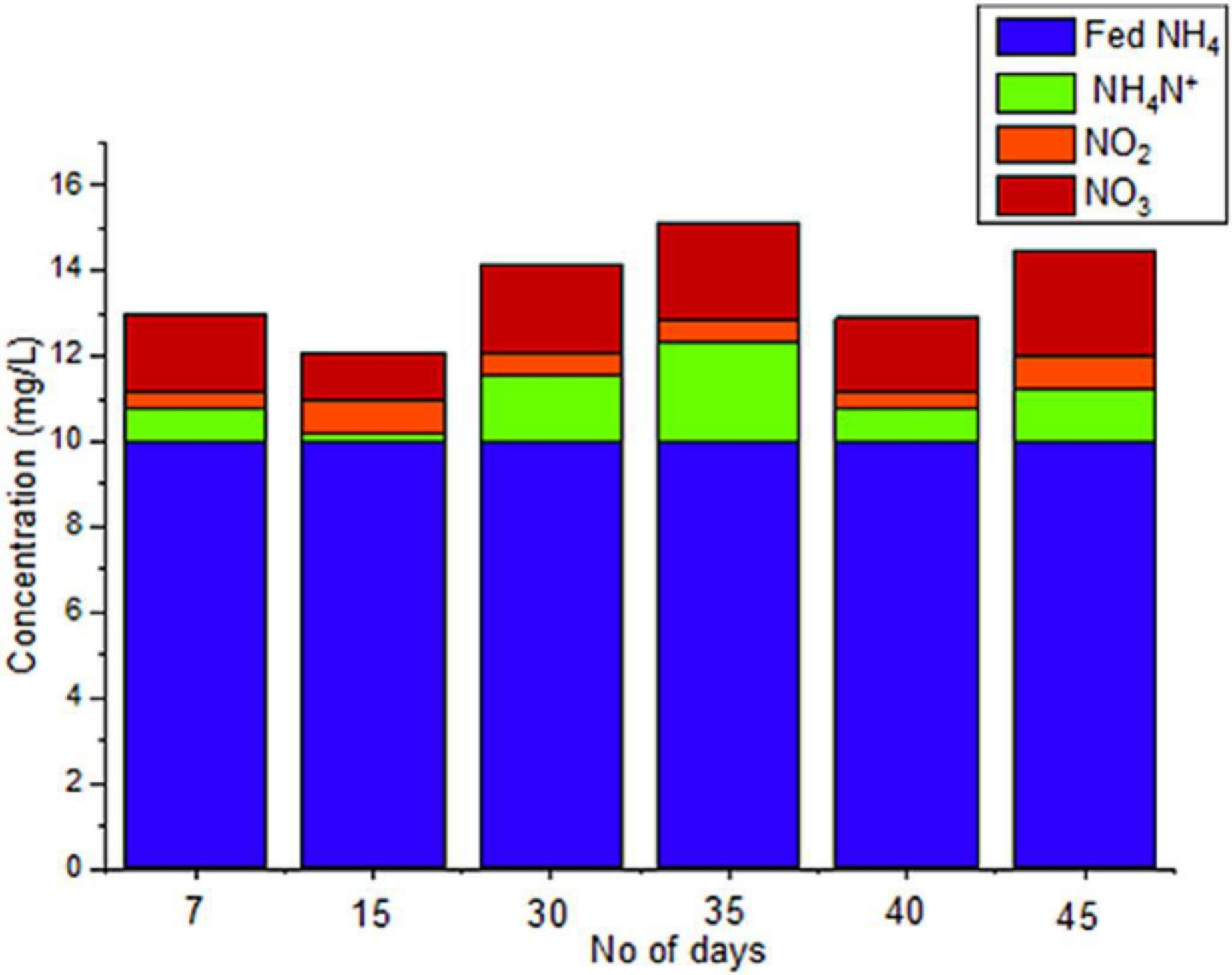
Fed NH4
NH4N+
NO2
NO3
Concentration (mg/L)
0
2
4
6
8
10
12
14
16
7
15
30
35
40
45
No of days

Figure 4

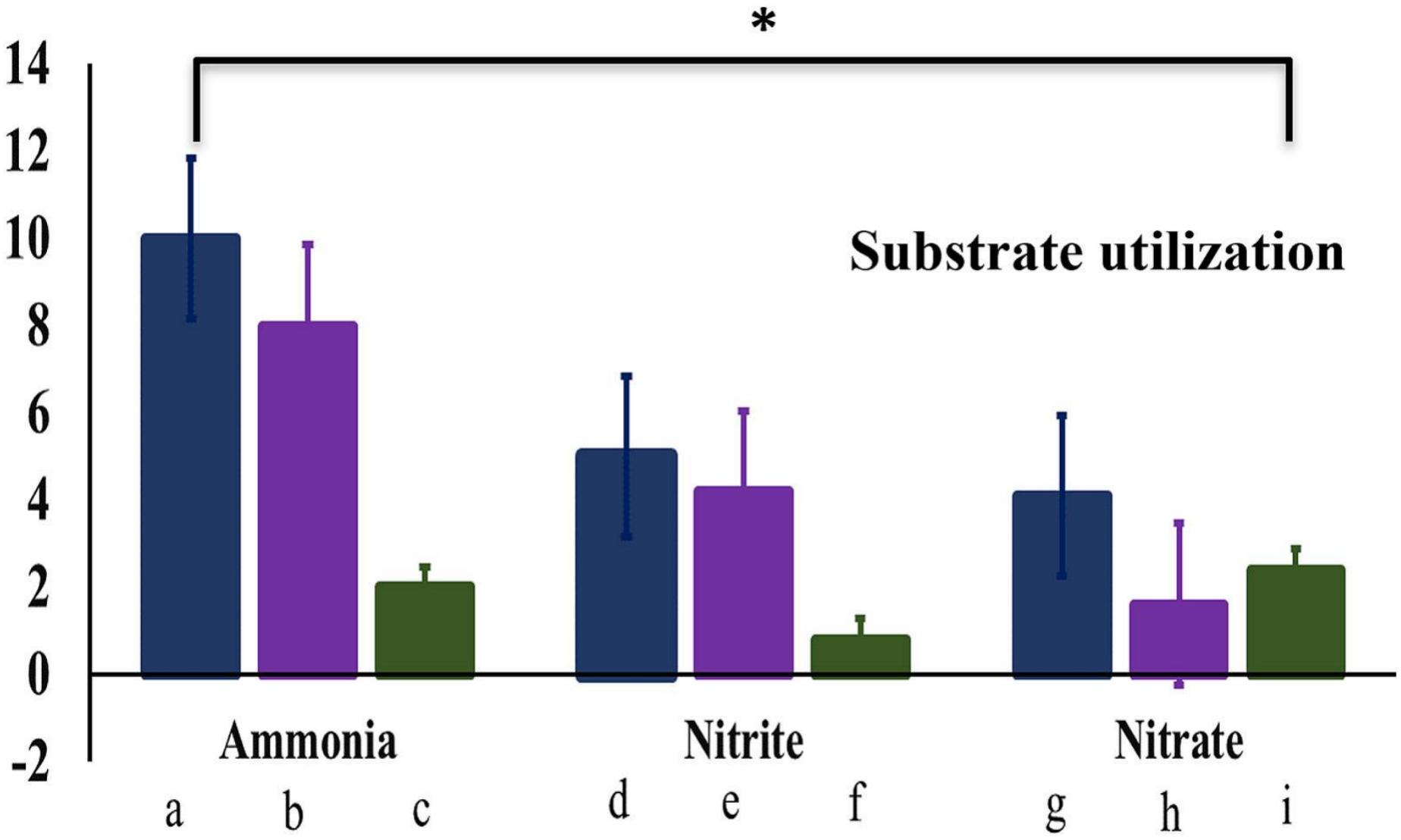
*
14
12
10
8
6
4
2
0
-2
Substrate utilization
Ammonia
Nitrite
Nitrate
a
b
c
d
e
f
g
h
i

Figure 5

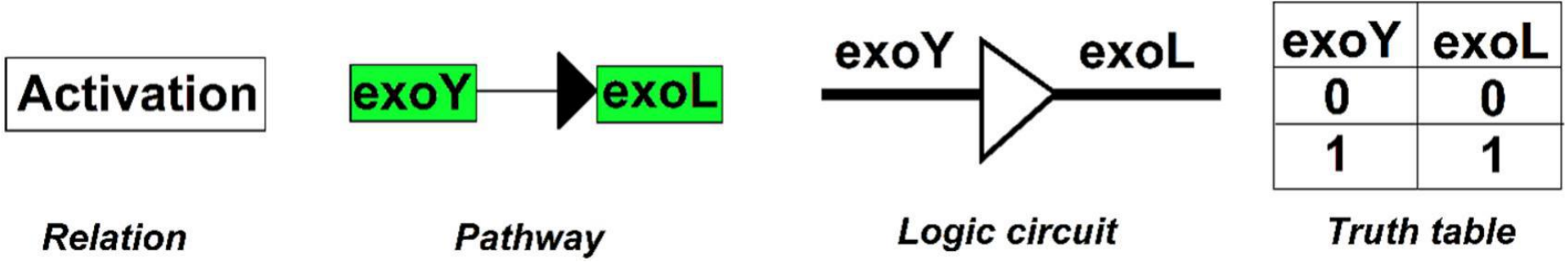
Activation
exoY
exoL
exoY
exoL
exoY
exoL
0
0
1
1
Relation
Pathway
Logic circuit
Truth table

Figure 6